



# Finite Volume discretization of flux-divergence in mapped grids with embedded boundaries

David Batista

August 2011

Publication Number: CSRCR2011-02

Computational Science &  
Engineering Faculty and Students  
Research Articles

Database Powered by the  
Computational Science Research Center  
Computing Group & Visualization Lab

## COMPUTATIONAL SCIENCE & ENGINEERING



**SAN DIEGO STATE  
UNIVERSITY**

Computational Science Research Center  
College of Sciences  
5500 Campanile Drive  
San Diego, CA 92182-1245  
(619) 594-3430



**Finite Volume discretization of flux-  
divergence in mapped grids with  
embedded boundaries**

**Report of Internship at Lawrence Berkeley National  
Laboratory, July 2010 - May 2011**

**By**

**David Batista  
Computational Science Research Center  
San Diego State University**

### **Acknowledgement:**

This work was done during my stay at LBNL in the Advanced Numerical Algorithms Group, from July 2010 to May 2011.

# FINITE VOLUME DISCRETIZATION OF FLUX-DIVERGENCE IN MAPPED GRIDS WITH EMBEDDED BOUNDARIES

DAVID BATISTA\*

## 1. Introduction.

The objective of this work is to construct a finite volume-based scheme for approximating the average of the divergence of a flux,  $\langle \nabla \cdot F \rangle$ , in curvilinear, non-boundary conforming grids, a case that we call: Mapped Embedded Boundary Method.

The two main contributions made are, first, the construction of an explicit formula for calculating multi-dimension derivatives of product of functions,  $\nabla^p(FG)$ , that allows us to do a detailed mathematical analysis of our approximating formulas while providing us with an efficient way of computationally evaluate  $\nabla^p(FG)$ . The second one is a mathematical proof of how, for these finite volume-based type of methods, just by taking Taylor expansions of fluxes we can obtain a conservative, high-order scheme but not a freestream one. On this regard, we show that integrals of rows of the matrix  $N$  associated with the mapping,  $\mathbf{X}$ , and given by:

$$(N^T)_{p,q} = \det((\nabla_{\xi} \mathbf{X})(p | \vec{e}^q)),$$

where  $A(p | \vec{v})$  is the matrix obtained by replacing the  $p^{th}$  row of the matrix  $A$  by the vector  $\vec{v}$ ,  $\vec{e}^d$  denotes the unit vector in the  $d^{th}$  coordinate direction; have "always" to be computed the right way in order to get a freestream preserving scheme. This is a general result that applies for the Cartesian Embedded Boundary and Mapped Finite Volume methods as well as for the Mapped Embedded Boundary method discussed here.

Finally, numerical results show that the schemes obtained are conservative, free-stream preserving, and produce high-order approximations of  $\langle \nabla \cdot F \rangle$  in two and three dimensions.

## 2. Preliminaries.

Let  $\mathbf{X}$  be a smooth map from the computational space  $[0, 1]^D$  to the physical space  $\Omega \subseteq \mathbb{R}^D$ ,

$$\mathbf{X} : [0, 1]^D \longrightarrow \Omega \subseteq \mathbb{R}^D,$$

$\xi \in [0, 1]^D$ ,  $\mathbf{X}(\xi) = (X_1(\xi), \dots, X_D(\xi))^T = x \in \Omega \subseteq \mathbb{R}^D$  and  $D$  represents the dimension of the spaces.

An irregular domain  $\Omega$  is discretized as a collection of control volumes (CV),  $V_i$ , obtained by intersecting  $\Omega$  with non-uniform, topologically cube (3D)/square (2D) grid cells. These non-uniform grid cells are considered to be the image over the

---

\*PhD Candidate. Computational Science Research Center, San Diego State University.

smooth mapping  $\mathbf{X}$  of cube/square grid cells defined on the computational space. Thus:

$$\mathbf{X}(V_i) = \mathbf{X}(\Upsilon_i) \cap \Omega,$$

where  $\Upsilon_i = [(\mathbf{i} - \frac{1}{2}\mathbf{u})h, (\mathbf{i} + \frac{1}{2}\mathbf{u})h]$ ,  $\mathbf{i} \in \mathbb{Z}^D$ ,  $h$  is the mesh spacing, and  $\mathbf{u}$  is the vector whose entries are all ones.

Each CV is classified as: *outside CV*, if it is a control volume that does not intersect  $\Omega$  ( $\mathbf{X}(\Upsilon_i) \cap \Omega = \emptyset$ ); *inside CV*, if it is a control volume completely contained in  $\Omega$  ( $\mathbf{X}(\Upsilon_i) \cap \Omega = \mathbf{X}(\Upsilon_i)$ ); and *irregular CV*, if it is neither an inside or outside CV. This classification of control volumes will also be used in the case of a Cartesian grid, that is, we will have *outside*, *inside* and *irregular* control volumes in the computational space as well as in the physical space. Furthermore, it is assumed that  $\mathbf{X}$  establishes a correspondence between control volumes of the same type.

An embedded boundary (EB) method is an algorithm developed for solving partial differential equations (PDE's) on complex domains discretized by a set of CVs. When the discretization of  $\Omega$  doesn't have irregular CV's we say we have a boundary conforming mesh and a Finite Volume (FV) algorithm for solving PDE's.

The particular case when the control volumes are cubes/squares, (Cartesian EB method or Cartesian FV method) is obtained by taking  $\mathbf{X}$  to be the identity map, that is,

$$V_i = \Upsilon_i \cap \Omega$$

We show how to construct high-order, multi-dimensional, conservative, free-stream preserving, finite volume-based approximations for calculating the average of the divergence of a flux in a curvilinear embedded boundary setting. This formulation is quite general and schemes for all other cases namely, Finite Volume, Cartesian EB, and Mapped FV, can be obtained from it while preserving/inheriting all its conservative properties and accuracy.

### 3. The basic equation for the average of the divergence of a flux.

By using the chain rule, Cramer's rule and the equality of mixed partial derivatives, the divergence of a flux,  $\nabla_x \cdot F$ , in the physical space can be written as ([1])

$$\nabla_x \cdot F = \frac{1}{J} \nabla_\xi \cdot (N^T F), \quad (3.1)$$

where  $J = \det(\nabla_\xi \mathbf{X})$ ,  $(N^T)_{p,q} = \det((\nabla_\xi \mathbf{X})(p | \vec{e}^q))$ ,  $A(p | \vec{v})$  is the matrix obtained by replacing the  $p^{th}$  row of the matrix  $A$  by the vector  $\vec{v}$ ,  $\vec{e}^d$  denotes the unit vector in the  $d^{th}$  coordinate direction, and  $F(x) = F(\mathbf{X}(\xi)) = F(\xi)$ .

We would like to discretize/approximate the average of the divergence of a flux,  $\langle \nabla_x \cdot F \rangle$ .

Let's consider an irregular control volume,  $\mathbf{X}(V_i) \subset \Omega$ , and the corresponding irregular control volume,  $V_i$ , in the computational space. From (3.1) it is obtained

$$\int_{\mathbf{X}(V_i)} \nabla_x \cdot F \, dx = \int_{V_i} \nabla_\xi \cdot (N^T F) \, d\xi,$$

and, therefore,  $\langle \nabla_x \cdot F \rangle$  is given by

$$\langle \nabla_x \cdot F \rangle = \frac{1}{|\mathbf{X}(V_i)|} \int_{V_i} \nabla_\xi \cdot (N^T F) \, d\xi, \quad (3.2)$$

We'll focus on discretizing the integral on the right hand side of (3.2), since

$$|\mathbf{X}(V_i)| = \frac{1}{D} \int_{V_i} \nabla_\xi \cdot (N^T F) \, d\xi,$$

when taking  $F(\xi) = \mathbf{X}(\xi)$ .

From the divergence theorem applied to the integral on the right hand side of (3.2) we get

$$\int_{V_i} \nabla_\xi \cdot (N^T F) \, d\xi = \sum_{d=0}^{D-1} \sum_{\pm=+,-} \pm \int_{A_\pm^d} (N^T F)_d \, dA_\xi + \int_{A_{EB}} (N^T F) \cdot \hat{n} \, d\xi \quad (3.3)$$

$A_\pm^d$  are the coordinate faces of the control volume  $V_i$ ,  $A_{EB}$  is the surface obtained by intersecting the domain with the Cartesian cell number  $i$ , and  $\hat{n}$  is the normal vector to  $A_{EB}$ .

#### 4. Discretizing equation (3.3).

In this section we present one of the main contribution of this work which is proving, mathematically, why by using just Taylor expansions on equation (3.3) we can get a high-order scheme but not a freestream preserving one. A way of fixing this problem is proposed.

In (3.3) we have written the integral  $\int_{V_i} \nabla_\xi \cdot (N^T F) \, d\xi$  over the whole control volume  $V_i$  in terms of integrals over its boundary,  $\partial V_i$ , and thus, the accuracy of our resulting scheme will depend on how precise our approximations of these integrals are. For achieving the desired high-order accuracy we use Taylor expansions of the vector function  $N^T F$ .

For the sake of conservation, we Taylor expand  $N^T F$  in the integrals over  $A_\pm^d$  and  $A_{EB}$ , about the face centroids  $\xi_\pm^d$  and  $\xi_{EB}$ , respectively, to get

$$\begin{aligned}
\int_{V_i} \nabla_\xi \cdot (N^T \mathbf{F}) d\xi &= \sum_{d=0}^{D-1} \sum_{\pm=+,-} \pm \int_{A_\pm^d} \sum_{0 \leq |p| \leq P} \frac{1}{p!} (\xi - \xi_\pm^d)^p \nabla^p (N^T \mathbf{F})_d(\xi_\pm^d) dA_\xi \\
&+ \int_{A_{EB}} \sum_{0 \leq |p| \leq P} \frac{1}{p!} (\xi - \xi_{EB})^p \left[ \sum_{s=0}^{D-1} \nabla^p (N^T \mathbf{F})_s(\xi_{EB}) \hat{n}_s \right] dA_\xi \\
&+ O(h^{P+D}) \tag{4.1}
\end{aligned}$$

We will denote by  $I_\pm^d$  the integral over  $A_\pm^d$  and by  $I_{EB}$  the integral over  $A_{EB}$ .

On the other hand, the multi-dimension derivatives,  $\nabla^p (N^T \mathbf{F})_s(\xi)$ , can be computed using the exact formula (see section 5.2):

$$\nabla^p (N^T \mathbf{F})_s(\xi) = \sum_{j=0}^{D-1} \sum_{0 \leq |q| \leq |p|} K_q \nabla^{p-q} \mathbf{F}_j(\xi) \nabla^q N_{s_j}^T(\xi), \tag{4.2}$$

Expression (4.2) is obtained by combining ideas from the Binomial theorem and combinatorics and its importance is two folded: (a) it provides us with a tool to mathematically manipulate expression (4.1) and (b) it allows us to easily and efficiently evaluate  $\nabla^p (N^T \mathbf{F})_s(\xi)$ .

To simplify the notation, we re-write equation (4.2) in a compact way as

$$\nabla^p (N^T \mathbf{F})_s(\xi) = \sum_{\substack{j=0, \dots, D-1 \\ 0 \leq |q| \leq |p|}} K_q \nabla^{p-q, q}(\mathbf{F}_j, N_{s_j}^T)(\xi), \tag{4.3}$$

where  $\nabla^{p-q, q}(\mathbf{F}_j, N_{s_j}^T)(\xi)$  is equal to the product  $\nabla^{p-q} \mathbf{F}_j(\xi) \nabla^q N_{s_j}^T(\xi)$ .  $K_q$  is the number of multi-indices  $q$  contained in  $p$ .

Then, the integral  $I_\pm^d$  can be written as:

$$\begin{aligned}
I_\pm^d &= \int_{A_\pm^d} \sum_{0 \leq |p| \leq P} \frac{1}{p!} (\xi - \xi_\pm^d)^p \sum_{\substack{j=0, \dots, D-1 \\ 0 \leq |q| \leq |p|}} K_q \nabla^{p-q, q}(\mathbf{F}_j, N_{d_j}^T)(\xi_\pm^d) dA_\xi \\
I_\pm^d &= \int_{A_\pm^d} \sum_{1 \leq |p| \leq P} \frac{1}{p!} (\xi - \xi_\pm^d)^p \sum_{\substack{j=0, \dots, D-1 \\ 0 \leq |q| \leq |p|-1}} K_q \nabla^{p-q, q}(\mathbf{F}_j, N_{d_j}^T)(\xi_\pm^d) dA_\xi \\
&+ \int_{A_\pm^d} \sum_{0 \leq |p| \leq P} \frac{1}{p!} (\xi - \xi_\pm^d)^p \sum_{j=0}^{D-1} \mathbf{F}_j(\xi_\pm^d) \nabla^p N_{d_j}^T(\xi_\pm^d) dA_\xi \tag{4.4}
\end{aligned}$$

The integral  $I_{EB}$  can be written as follows

$$I_{EB} = \int_{A_{EB}} \sum_{s=0}^{D-1} \left[ \sum_{1 \leq |p| \leq P} \frac{1}{p!} (\xi - \xi_{EB})^p \sum_{\substack{j=0, \dots, D-1 \\ 0 \leq |q| \leq |p|-1}} K_q \nabla^{p-q, q} (\mathbf{F}_j, N_{s,j}^T)(\xi_{EB}) \right] \hat{n}_s dA_\xi \\ + \int_{A_{EB}} \sum_{s=0}^{D-1} \left[ \sum_{0 \leq |p| \leq P} \frac{1}{p!} (\xi - \xi_{EB})^p \sum_{j=0}^{D-1} \mathbf{F}_j(\xi_{EB}) \nabla^p N_{s,j}^T(\xi_{EB}) \right] \hat{n}_s dA_\xi \quad (4.5)$$

By substituting (4.4) and (4.5) into (4.1) it is obtained

$$\int_{V_i} \nabla_\xi \cdot (N^T \mathbf{F}) d\xi = \quad (4.6)$$

$$\sum_{d=0}^{D-1} \sum_{\pm=+,-} \pm \left[ \int_{A_\pm^d} \sum_{1 \leq |p| \leq P} \frac{1}{p!} (\xi - \xi_\pm^d)^p \sum_{\substack{j=0, \dots, D-1 \\ 0 \leq |q| \leq |p|-1}} K_q \nabla^{p-q, q} (\mathbf{F}_j, N_{d,j}^T)(\xi_\pm^d) dA_\xi \right] \quad (4.6.a)$$

$$+ \left[ \int_{A_\pm^d} \sum_{0 \leq |p| \leq P} \frac{1}{p!} (\xi - \xi_\pm^d)^p \sum_{j=0}^{D-1} \mathbf{F}_j(\xi_\pm^d) \nabla^p N_{d,j}^T(\xi_\pm^d) dA_\xi \right] \quad (4.6.b)$$

$$+ \sum_{s=0}^{D-1} \int_{A_{EB}} \left[ \sum_{1 \leq |p| \leq P} \frac{1}{p!} (\xi - \xi_{EB})^p \sum_{\substack{j=0, \dots, D-1 \\ 0 \leq |q| \leq |p|-1}} K_q \nabla^{p-q, q} (\mathbf{F}_j, N_{s,j}^T)(\xi_{EB}) \right] \hat{n}_s dA_\xi \quad (4.6.c)$$

$$+ \int_{A_{EB}} \sum_{s=0}^{D-1} \left[ \sum_{0 \leq |p| \leq P} \frac{1}{p!} (\xi - \xi_{EB})^p \sum_{j=0}^{D-1} \mathbf{F}_j(\xi_{EB}) \nabla^p N_{s,j}^T(\xi_{EB}) \right] \hat{n}_s dA_\xi \quad (4.6.d)$$

$$+ O(h^{P+D})$$

Let's examine (4.6.b) and (4.6.d).

$$(4.6.b) = \sum_{j=0}^{D-1} \left[ \mathbf{F}_j(\xi_\pm^d) \int_{A_\pm^d} \sum_{0 \leq |p| \leq P} \frac{1}{p!} (\xi - \xi_\pm^d)^p \nabla^p N_{d,j}^T(\xi_\pm^d) dA_\xi \right] \\ = \sum_{j=0}^{D-1} \left[ \mathbf{F}_j(\xi_\pm^d) \int_{A_\pm^d} \sum_{0 \leq |p| \leq P} \frac{1}{p!} (\xi - \xi_\pm^d)^p \nabla^p N_{j,d}(\xi_\pm^d) dA_\xi \right] \\ = \sum_{j=0}^{D-1} \left[ \mathbf{F}_j(\xi_\pm^d) \int_{A_\pm^d} T_{\xi_\pm^d}^P N_{j,d}(\xi) dA_\xi \right], \quad (4.7)$$

where  $T_{\xi_\pm^d}^P N_{j,d}(\xi)$  is the  $P$ -th order Taylor polynomial of  $N_{j,d}$  about  $\xi_\pm^d$ .

Analogously, (4.6.d) is equal to

$$(4.6.d) = \sum_{j=0}^{D-1} \left[ \mathbf{F}_j(\xi_{EB}) \int_{A_{EB}} \sum_{s=0}^{D-1} [T_{\xi_{EB}}^P N_{j s}(\xi)] \hat{n}_s dA_\xi \right], \quad (4.8)$$

(4.7) and (4.8) are the freestream destroyers, as it is explained next.

By substituting (4.7) and (4.8) into (4.6) it is obtained:

$$\int_{V_i} \nabla_\xi \cdot (N^T \mathbf{F}) d\xi = \quad (4.9)$$

$$\sum_{d=0}^{D-1} \sum_{\pm=+,-} \pm \left[ \int_{A_\pm^d} \sum_{1 \leq |p| \leq P} \frac{1}{p!} (\xi - \xi_\pm^d)^p \sum_{\substack{j=0, \dots, D-1 \\ 0 \leq |q| \leq |p|-1}} K_q \nabla^{p-q, q}(\mathbf{F}_j, N_{d j}^T)(\xi_\pm^d) dA_\xi \right] \quad (4.9.a)$$

$$+ \sum_{j=0}^{D-1} \mathbf{F}_j(\xi_\pm^d) \int_{A_\pm^d} T_{\xi_\pm^d}^P N_{j d}(\xi) dA_\xi \quad (4.9.b)$$

$$+ \sum_{s=0}^{D-1} \int_{A_{EB}} \left[ \sum_{1 \leq |p| \leq P} \frac{1}{p!} (\xi - \xi_{EB})^p \sum_{\substack{j=0, \dots, D-1 \\ 0 \leq |q| \leq |p|-1}} K_q \nabla^{p-q, q}(\mathbf{F}_j, N_{s j}^T)(\xi_{EB}) \right] \hat{n}_s dA_\xi \quad (4.9.c)$$

$$+ \sum_{j=0}^{D-1} \left[ \mathbf{F}_j(\xi_{EB}) \int_{A_{EB}} \sum_{s=0}^{D-1} T_{\xi_{EB}}^P N_{j s}(\xi) \right] \hat{n}_s dA_\xi \quad (4.9.d)$$

$$+ O(h^{P+D})$$

Suppose  $\mathbf{F}(\xi) = C$  is a constant flux. If derivatives  $\nabla^p \mathbf{F}_j$  are approximated appropriately, i.e. by using a linear combination of values of  $\mathbf{F}_j$ ,  $\sum_{k \in K} \alpha_k \mathbf{F}_j^k$ , such as  $\sum_{k \in K} \alpha_k = 0$  then, (4.9.a) and (4.9.c) are equal to zero, because sums over  $|p|$  start at 1. Thus, (4.9) becomes:

$$\int_{V_i} \nabla_\xi \cdot (N^T \mathbf{F}) d\xi = \sum_{j=0}^{D-1} C_j \left[ \sum_{d=0}^{D-1} \sum_{\pm} \pm \int_{A_\pm^d} T_{\xi_\pm^d}^P N_{j d}(\xi) dA_\xi + \int_{A_{EB}} \sum_{s=0}^{D-1} (T_{\xi_{EB}}^P N_{j s}(\xi)) \hat{n}_s dA_\xi \right]$$

Obs: The error term  $O(h^{P+D})$  in equation (4.9) is equal to zero because it is proportional to some derivative of  $\mathbf{F}$ , and  $\mathbf{F}$  is constant.

Since,  $N_{j d}(\xi) = T_{\xi_\pm^d}^P N_{j d}(\xi) + O(h^{P+1})$  and  $N_{j s}(\xi) = T_{\xi_{EB}}^P N_{j s}(\xi) + O(h^{P+1})$ , we get

$$\begin{aligned} \int_{V_i} \nabla_\xi \cdot (N^T \mathbf{F}) d\xi = & \\ & \sum_{j=0}^{D-1} C_j \left[ \sum_{d=0}^{D-1} \sum_{\pm} \pm \int_{A_{\pm}^d} N_{j,d}(\xi) dA_\xi + \int_{A_{EB}} (N(\xi) \cdot \hat{n}_s)_j dA_\xi \right] \\ & + O(h^{P+D}) \end{aligned}$$

$$\int_{V_i} \nabla_\xi \cdot (N^T \mathbf{F}) d\xi = \sum_{j=0}^{D-1} C_j \left[ \int_{V_i} \nabla_\xi \cdot (N_{j,\bullet}) d\xi \right] + O(h^{P+D}),$$

where  $N_{j,\bullet}$  is the row  $j$  of  $N$ .

Since each row of  $N$  is divergence free (which can be checked by direct computation), we finally get,

$$\int_{V_i} \nabla_\xi \cdot (N^T \mathbf{F}) d\xi = O(h^{P+D}), \quad (4.10)$$

Thus, we fail to satisfy the freestream preserving property because we are calculating integrals  $\int_{A_{\pm}^d} N_{j,d}(\xi) dA_\xi$  and  $\int_{A_{EB}} (N(\xi) \cdot \hat{n})_j dA_\xi$  inappropriately, namely, by using Taylor expansions. By doing so, the condition that rows of  $N$  are divergence free is not fulfilled which introduces an error of order  $O(h^{P+D})$  into the formulation that, otherwise, would be freestream preserving already (in terms of flux calculations).

This analysis is not restricted to the mapped-EB case. In fact, it is a very general result that works for the Finite Volume, Mapped Finite Volume, Cartesian EB, and Mapped EB methods.

Figure 4.1 shows an example of this phenomenon. We have implemented a Mapped FV, second order version of equation (4.9) and tested it for a constant flux. As predicted, we do not get exact zero but an error that, in this case, is second order.

In order to get a freestream preserving scheme we proceed as follows.

Going bak to (4.9), let's substitute the approximate values  $\int_{A_{\pm}^d} T_{\xi_{\pm}^d}^P N_{j,d}(\xi) dA_\xi$  and  $\int_{A_{EB}} \sum_{s=0}^{D-1} \left( T_{\xi_{EB}}^P N_{j,s}(\xi) \right) \hat{n}_s dA_\xi$  by the exact values  $\int_{A_{\pm}^d} N_{j,d}(\xi) dA_\xi$  and  $\int_{A_{EB}} (N(\xi) \cdot \hat{n})_j dA_\xi$ , respectively.

As seen in (4.10) this introduces an error  $O(h^{P+D})$  but, the error in (4.9) is  $O(h^{P+D})$  thus, the total error doesn't change.

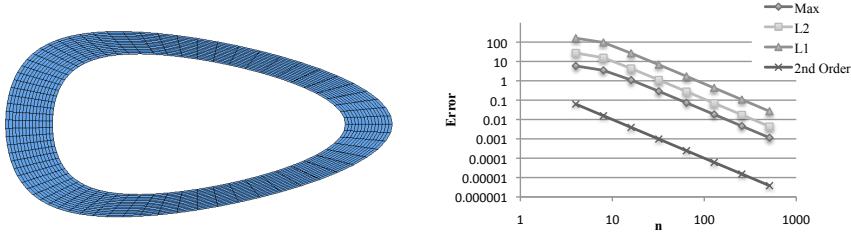


FIG. 4.1. *No freestream preservation for the Mapped FV case. Left: boundary conforming curvilinear grid, right: error obtained. This error is different than zero and, therefore, the scheme is not freestream preserving*

Then,

$$\int_{V_i} \nabla_{\xi} \cdot (N^T \mathbf{F}) d\xi = \quad (4.11)$$

$$\sum_{d=0}^{D-1} \sum_{\pm=+,-} \pm \left[ \int_{A_{\pm}^d} \sum_{1 \leq |p| \leq P} \frac{1}{p!} (\xi - \xi_{\pm}^d)^p \sum_{\substack{j=0, \dots, D-1 \\ 0 \leq |q| \leq |p|-1}} K_q \nabla^{p-q, q} (\mathbf{F}_j, N_{d,j}^T)(\xi_{\pm}^d) dA_{\xi} \right] \quad (4.11.a)$$

$$+ \sum_{j=0}^{D-1} \mathbf{F}_j(\xi_{\pm}^d) \int_{A_{\pm}^d} N_{j,d}(\xi) dA_{\xi} \quad (4.11.b)$$

$$+ \sum_{s=0}^{D-1} \int_{A_{EB}} \left[ \sum_{1 \leq |p| \leq P} \frac{1}{p!} (\xi - \xi_{EB})^p \sum_{\substack{j=0, \dots, D-1 \\ 0 \leq |q| \leq |p|-1}} K_q \nabla^{p-q, q} (\mathbf{F}_j, N_{s,j}^T)(\xi_{EB}) \right] \hat{n}_s dA_{\xi} \quad (4.11.c)$$

$$+ \sum_{j=0}^{D-1} \left[ \mathbf{F}_j(\xi_{EB}) \int_{A_{EB}} (N(\xi) \hat{n})_j dA_{\xi} \right] \quad (4.11.d)$$

$$+ O(h^{P+D})$$

When  $|A_{EB}|$  goes to zero, (4.11.c) and (4.11.d) also go to zero because they are integrals over  $A_{EB}$  and we recover formulas in [1].

As a summary: right after applying the Divergence theorem to the integral in (3.2) we have taken Taylor expansions of  $(N^T(\xi) \mathbf{F}(\xi))_d$  in (3.3). By using the exact, new formula for calculating multi-dimensional derivatives (equation (4.3)), we have

rearranged terms to show that integrals of the divergence of rows of  $N$  have "always" to be calculated in an appropriate way for guarantying freestream; a computation that was hidden in the formulation. Thus, computing the integrals  $\int_{A_{\pm}^d} N_{j d}(\xi) dA_{\xi}$  and  $\int_{A_{EB}} (N(\xi) \hat{n})_j dA_{\xi}$  appears in a natural way. For a given control volume  $V_i$ , equation (4.11) provides an explicit formula for computing the integral  $\int_{V_i} \nabla_{\xi} \cdot (N^T F) d\xi$  up to any order of accuracy.

The standard Finite Volume case is obtained when having a boundary conforming, Cartesian grid. In this scenario the map,  $\mathbf{X}$ , and, therefore, the matrix,  $N$ , are the identity operators. The integral  $\int_{A_{\pm}^d} N_{j d}(\xi) dA_{\xi}$  is either zero or equal to  $|A_{\pm}^d|$  and the divergence free condition of the rows of  $N$  gets trivially satisfied thanks to the topological symmetries of the problem. For all the other cases, we have to calculate the integrals  $\int_{A_{\pm}^d} N_{j d}(\xi) dA_{\xi}$  and  $\int_{A_{EB}} (N(\xi) \hat{n})_j dA_{\xi}$  in an appropriate way. In section (5.3) we show how to do so using the ideas presented in [1].

## 5. Implementation of equation (4.11).

In this section we show some details about the implementation of formula (4.11), specifically, we show how to compute integrals of the form  $\int_{A_{\pm}^d} (\xi - \xi_0)^p dA$ , or moments, how to compute multi-dimension derivatives of product of vector functions,  $\nabla^p (N^T F)_s(\xi)$ , and how to calculate the integrals  $\int_{A_{\pm}^d} N_{j d} dA_{\xi}$  and  $\int_{A_{EB}} (N \hat{n})_j dA_{\xi}$  in order to get freestream preservation.

### 5.1. Computing integrals of the form $\int_{A_{\pm}^d} (\xi - \xi_0)^p dA$ .

Integrals of the form

$$\int_{\tilde{A}_{\pm}^d} \xi_0^{p_0} \xi_1^{p_1} \dots \xi_{D-1}^{p_{D-1}} d\tilde{A} = \int_{\tilde{A}_{\pm}^d} \xi^p d\tilde{A}, \quad (5.1)$$

where  $\xi = (\xi_0, \xi_1, \dots, \xi_{D-1}) \in \mathbb{R}^D$  and  $p = (p_0, p_1, \dots, p_{D-1}) \in \mathbb{N}^D$  is a multi-index, are called "moments".

The region  $\tilde{A}_{\pm}^d$  is given by:  $\tilde{A}_{\pm}^d = T(A_{\pm}^d)$ , where  $T(\xi) = \xi - \xi^c$  and  $\xi^c \in \mathbb{R}^D$  is the center of the control volume  $V_i$  that is, moments are calculated using local coordinates, where the center of the cell is taken to be the zero vector.

The integrals (5.1) are already computed and we will use them to calculate

$$\int_{A_{\pm}^d} (\xi - \xi_0)^p dA, \quad (5.2)$$

for any given  $\xi_0 \in \mathbb{R}^D$  and any  $p \in \mathbb{N}^D$ . Integral (5.2) appears when we Taylor-expand fluxes during the discretization process.

Adding to and subtracting from the integrand in (5.2), the vector  $\xi^c$ , we get:

$$\int_{A_{\pm}^d} (\xi - \xi_0)^p dA = \int_{A_{\pm}^d} (\xi - \xi^c + \xi^c - \xi_0)^p dA = \int_{\tilde{A}_{\pm}^d} (\zeta + \xi_1)^p d\tilde{A}, \quad (5.3)$$

with  $\zeta = \xi - \xi^c$  and  $\xi_1 = \xi^c - \xi_0$ .

Now, by definition,  $(\zeta + \xi_1)^p$  is written as

$$(\zeta + \xi_1)^p = \prod_{j=0}^{D-1} (\zeta_j + \xi_j^1)^{p_j}, \quad (5.4)$$

where each factor can be computed as follows

$$(\zeta_j + \xi_j^1)^{p_j} = \sum_{k_j=0}^{p_j} \binom{p_j}{k_j} \zeta_j^{k_j} (\xi_j^1)^{p_j-k_j} \quad (5.5)$$

Combining (5.5) and (5.4) it is obtained

$$(\zeta + \xi_1)^p = \prod_{j=0}^{D-1} \left( \sum_{k_j=0}^{p_j} \binom{p_j}{k_j} \zeta_j^{k_j} (\xi_j^1)^{p_j-k_j} \right) \quad (5.6)$$

After algebraic manipulations, (5.6) can be written as

$$\begin{aligned} (\zeta + \xi_1)^p = & \sum_{k_0=0}^{p_0} \binom{p_0}{k_0} (\xi_0^1)^{p_0-k_0} \left[ \sum_{k_1=0}^{p_1} \binom{p_1}{k_1} (\xi_1^1)^{p_1-k_1} \left[ \dots \right. \right. \\ & \left. \left. \left[ \sum_{k_{D-1}=0}^{p_{D-1}} \binom{p_{D-1}}{k_{D-1}} (\xi_{D-1}^1)^{p_{D-1}-k_{D-1}} \left[ \zeta_0^{k_0} \zeta_1^{k_1} \dots \zeta_{D-1}^{k_{D-1}} \right] \dots \right] \right] \end{aligned} \quad (5.7)$$

Integrating (5.7) over  $\tilde{A}_{\pm}^d$  produces

$$\begin{aligned} \int_{\tilde{A}_{\pm}^d} (\zeta + \xi_1)^p dA = & \sum_{k_0=0}^{p_0} \binom{p_0}{k_0} (\xi_0^1)^{p_0-k_0} \left[ \sum_{k_1=0}^{p_1} \binom{p_1}{k_1} (\xi_1^1)^{p_1-k_1} \left[ \dots \right. \right. \\ & \left. \left. \left[ \sum_{k_{D-1}=0}^{p_{D-1}} \binom{p_{D-1}}{k_{D-1}} (\xi_{D-1}^1)^{p_{D-1}-k_{D-1}} \left[ \int_{\tilde{A}_{\pm}^d} \zeta_0^{k_0} \zeta_1^{k_1} \dots \zeta_{D-1}^{k_{D-1}} d\tilde{A} \right] \dots \right] \right] \end{aligned}$$

or, equivalently,

$$\int_{A_{\pm}^d} (\xi - \xi_0)^p dA = \sum_{k_0=0}^{p_0} \binom{p_0}{k_0} (\xi_0^1)^{p_0-k_0} \left[ \sum_{k_1=0}^{p_1} \binom{p_1}{k_1} (\xi_1^1)^{p_1-k_1} \left[ \dots \right. \right. \\ \left. \left. \left[ \sum_{k_{D-1}=0}^{p_{D-1}} \binom{p_{D-1}}{k_{D-1}} (\xi_{D-1}^1)^{p_{D-1}-k_{D-1}} \left[ \int_{\tilde{A}_{\pm}^d} \zeta_0^{k_0} \zeta_1^{k_1} \dots \zeta_{D-1}^{k_{D-1}} d\tilde{A} \right] \right] \dots \right] \right] \quad (5.8)$$

As we can see in (5.8), for a given  $j$ ,  $0 \leq j < D-1$ , each of the sums is of the form

$$\text{Sum}^j = \sum_{k_j=0}^{p_j} \binom{p_j}{k_j} (-\xi_j^0)^{p_j-k_j} \left( \text{Sum}^{j+1} \right)$$

For  $j = D-1$  we have that

$$\text{Sum}^{D-1} = \sum_{k_{D-1}=0}^{p_{D-1}} \binom{p_{D-1}}{k_{D-1}} (-\xi_{D-1}^0)^{p_{D-1}-k_{D-1}} \left[ \int_{\tilde{A}_{\pm}^d} \zeta_0^{k_0} \zeta_1^{k_1} \dots \zeta_{D-1}^{k_{D-1}} d\tilde{A} \right]$$

Expression (5.8) has been implemented recursively, finishing the recursion when  $j = D-1$ , by asking for the (already computed) moment  $\int_{\tilde{A}_{\pm}^d} \zeta_0^{k_0} \zeta_1^{k_1} \dots \zeta_{D-1}^{k_{D-1}} d\tilde{A}$ .

The case

$$\int_{A_{\pm}^d} (\xi - \xi_0)^p (\xi - \nu_0)^q dA,$$

with  $\xi, \xi_0, \nu_0 \in \mathbb{R}^D$  and multi-indices  $p, q \in \mathbb{N}^D$ , appears when Taylor-expanding the normal vector,  $\hat{n}$ , in (4.11) and can be calculated according to:

$$\int_{A_{\pm}^d} (\xi - \xi_0)^p (\xi - \nu_0)^q dA = \sum_{k_0=0}^{p_0} \binom{p_0}{k_0} (\xi_0^1)^{p_0-k_0} \left[ \sum_{k_1=0}^{p_1} \binom{p_1}{k_1} (\xi_1^1)^{p_1-k_1} \left[ \dots \right. \right. \\ \left. \left. \left[ \sum_{k_{D-1}=0}^{p_{D-1}} \binom{p_{D-1}}{k_{D-1}} (\xi_{D-1}^1)^{p_{D-1}-k_{D-1}} \left[ \sum_{r_0=0}^{q_0} \binom{q_0}{r_0} (\nu_0^1)^{q_0-r_0} \left[ \dots \right. \right. \right. \right. \\ \left. \left. \left. \left[ \sum_{r_{D-1}=0}^{q_{D-1}} \binom{q_{D-1}}{r_{D-1}} (\nu_{D-1}^1)^{q_{D-1}-r_{D-1}} \left[ \int_{\tilde{A}_{\pm}^d} \zeta_0^{k_0+r_0} \zeta_1^{k_1+r_1} \dots \zeta_{D-1}^{k_{D-1}+r_{D-1}} d\tilde{A} \right] \right] \dots \right] \right] \right] \right] \quad (5.9)$$

with  $\zeta = \xi - \xi^c$ ,  $\xi_1 = \xi^c - \xi_0$ , and  $\nu_1 = \xi^c - \nu_0$ .

## 5.2. Computing multi-dimension derivative $\nabla^p(N^T F)_s(\xi)$ .

We will denote the multi-dimension derivative of the product of two functions,  $F$  and  $G$ , by

$$\nabla^p (F(x) G(x)), \quad (5.10)$$

where  $F, G: \mathbb{R}^D \rightarrow \mathbb{R}$  are vector functions and  $p \in \mathbb{N}^D$  is a multi-index indicating the derivatives to be computed. For instance, the derivative

$$\frac{\partial^2}{\partial x^2} \frac{\partial}{\partial y} (F(x) G(x)), \quad (5.11)$$

is denoted by expression (5.10) with  $p = (2, 1)$ .

Inspired on the Binomial theorem and by using combinatorics we will write an exact formula to compute (5.10) for any dimension  $D \in \mathbb{N}$  and any multi-index  $p \in \mathbb{N}^D$ .

First, suppose the simplest case  $D = 1$ .

Let's compute, for instance, the derivative  $\frac{\partial^3}{\partial x^3} (F(x) G(x))$ . By direct computation and after grouping terms, we get:

$$\frac{\partial^3}{\partial x^3} (F G) = \frac{\partial^3 F}{\partial x^3} G + 3 \frac{\partial^2 F}{\partial x^2} \frac{\partial G}{\partial x} + 3 \frac{\partial F}{\partial x} \frac{\partial^2 G}{\partial x^2} + F \frac{\partial^3 G}{\partial x^3},$$

which, written in the form (5.10), is equal to:

$$\nabla^3 (F G) = \nabla^3 F \nabla^0 G + 3 \nabla^2 F \nabla^1 G + 3 \nabla^1 F \nabla^2 G + \nabla^0 F \nabla^3 G,$$

or,

$$\nabla^p (F G) = \sum_{0 \leq q \leq p} \binom{p}{q} \nabla^{p-q} F \nabla^q G, \quad (5.12)$$

with  $p = 3$ .

As we can see, (5.12) looks exactly like the Binomial theorem, where  $\binom{p}{q}$  counts how many distinct  $q$ -elements subsets, or  $q$ -subsets, we have in a set with  $p$  elements, or a  $p$ -set.

Now, let's compute (5.11). This is equal to:

$$\begin{aligned} \nabla^{(2,1)} (F G) = & \nabla^{(2,1)} F \nabla^{(0,0)} G + 2 \nabla^{(1,1)} F \nabla^{(1,0)} G + \\ & \nabla^{(2,0)} F \nabla^{(0,1)} G + 2 \nabla^{(1,0)} F \nabla^{(1,1)} G + \\ & \nabla^{(0,1)} F \nabla^{(2,0)} G + \nabla^{(0,0)} F \nabla^{(2,1)} G, \end{aligned}$$

or,

$$\nabla^p (FG) = \sum_{0 \leq |q| \leq |p|} K_q \nabla^{p-q} F \nabla^q G, \quad (5.13)$$

with  $p = (2, 1)$  and  $|p| = \sum_{j=0}^{D-1} p_j$ . Here, in general,  $K_q \neq \binom{p}{q}$ . Therefore, even though (5.13) looks like the Binomial theorem, it is not equal to (5.12). The reason why this happens is that, now,  $p$  and  $q$  are not just numbers but vectors of integers.

For the rest of this section we will refer to a vector of integers,  $p = (p_0, \dots, p_{D-1}) \in \mathbb{N}^D$ , either as the multi-index  $p$  or as the set  $p$  with  $p_0$  elements of some type,  $p_1$  elements of some other type, etc, and  $|p|$  elements in total. A multi-index  $q \in \mathbb{N}^D$ , is a subset of  $p$  if  $q_i \leq p_i$ , for every  $i = 0, \dots, D-1$ .

In expression (5.13),  $K_q$  is equal to the number of subsets,  $q$ , we have in  $p$  but now, we care about the subset  $q$  itself when counting for  $|q|$ -subsets of  $p$ . That is, we don't only have to count the subsets but to construct them as well.

Different multi-indices  $q^1, q^2$ , with the same modulus,  $|q^1| = |q^2|$ , can have different coefficients associated,  $K_{q^1} \neq K_{q^2}$ . Furthermore, some multi-indices,  $q$ , satisfying  $0 \leq |q| \leq |p|$ , might not be a subset of the multi-index  $p$ , e.g.  $q^1 = (2, 0)$  is a subset of  $p = (2, 1)$ , whereas  $q^2 = (0, 2)$  is not, even though  $|q^1| = |q^2| = 2 \leq 3 = |p|$ .

Every multi-index  $q$  and, therefore,  $p-q$ , is unique, meaning that there is "almost" no redundancy in (5.13). We say "almost" because, even though  $q^1 = (0, 1) \neq q^2 = (1, 1)$ , in both cases we have to compute  $\frac{\partial G}{\partial y}$ . The way (5.13) has been implemented we compute  $\nabla^{q^1} G$  and  $\nabla^{q^2} G$  separately thus, we could still have some room for improvements. However, the algorithm for (5.13) works recursively over multi-indices, calculating the derivatives  $\nabla^{p-q} F$  and  $\nabla^q G$  only once, at the end of the recursion. Since multi-indices are vectors of integers of length equal to  $D$  (the dimension of the problem), the algorithm is computationally efficient.

As we mention before, we want to count subsets of a given set. Two very common methods for enumerating the subsets of a given set are lexicographic ordering and Gray codes, neither of which is particularly well suited when looking for a minimum subset. These methods do not generate a sequence of subsets in which the number of elements in each subset increases monotonically. For our particular purpose, which is evaluating (5.13):

$$\nabla^p (FG) = \sum_{0 \leq |q| \leq |p|} K_q \nabla^{p-q} F \nabla^q G,$$

having an algorithm with this characteristic is important, for two main reasons:

1. Terms of the form  $\nabla^p(FG)$  appear on Taylor expansions of  $FG$  which, in turn, are used for discretizing flux-divergence. We use expression (5.13) for mathematical analysis of these flux-divergence numerical discretizations by, possibly, breaking the sum in (5.13), rearranging terms, etc. If subsets  $q$  are generated in a monotonically increasing fashion, the resulting mathematical

expressions can be evaluated with slight modifications (if any) of the original algorithm for computing (5.13).

2. Subsets  $q$  are multi-indices, which indicate what derivatives have to be computed. Generating them ordered by their size,  $|q|$ , means that we first evaluate all (if any) first order derivatives, then all (if any) second order derivatives, and so on. We could use this fact to eliminate all redundancy when computing  $\nabla^p(FG)$  by, let's say, saving previously calculated derivatives and reusing them later.

The idea of a  $k$ -subset of a set having  $n$  elements can be expressed by means of a  $n$ -digit binary number in which exactly  $k$  of the digits are 1. When  $k$ -subsets are enumerated before any  $(k+1)$ -subset we obtain the so called Banker's sequence. We have adapted the algorithm for generating a Banker's sequence presented in [2], that outputs the binary representation of a  $k$ -subset. With it, we construct the corresponding  $|q|$ -subset,  $q$ , of  $p$ , with  $|q| = k$ .

### 5.3. Computing integrals $\int_{A_{\pm}^d} N_{j,d} dA_{\xi}$ and $\int_{A_{EB}} (N \hat{n})_j dA_{\xi}$ .

In this section we show how to calculate the integrals

$$\int_{A_{\pm}^d} N_{j,d} dA_{\xi} \quad \text{and} \quad \int_{A_{EB}} (N \hat{n})_j dA_{\xi}$$

such as, we get a freestream preserving scheme from equation (4.11). For computing  $\int_{A_{\pm}^d} N_{j,d} dA_{\xi}$ , we follow the ideas presented in the Mapped Finite Volume case [1], which are based on the theory of differential forms and the use of Poincare Lemma. For the general case discuss here, we also have to calculate  $\int_{A_{EB}} (N \hat{n})_j dA_{\xi}$ . For doing so, we first apply the divergence theorem on the complement,  $\Upsilon_i - V_i$ , of the control volume  $V_i$  to write the integral over the EB-face in terms of integrals over coordinate faces and, then, we use Poincare Lemma again. This can be done because the mapping  $\mathbf{X}$  is defined over the rectangular control volumes  $\Upsilon_i$ ,  $i \in \mathbb{Z}^D$  and, therefore, so is the matrix  $N$ .

Any vector field  $\vec{v} = (v_0, \dots, v_{D-1})^T$  on  $\mathbb{R}^D$  has a corresponding  $(D-1)$ -form

$$w = v_0 (dx^1 \wedge dx^2 \wedge \dots \wedge dx^{D-1}) + \dots + (-1)^{D-1} v_{D-1} (dx^0 \wedge dx^1 \wedge \dots \wedge dx^{D-2}),$$

whose exterior derivative is the  $D$ -form

$$dw = \text{div}(\vec{v}) (dx^0 \wedge dx^1 \wedge \dots \wedge dx^{D-1}),$$

where  $\text{div}(\vec{v})$  is the divergence of  $\vec{v}$ .

The  $j^{\text{th}}$ -row of the matrix  $N$ ,  $N_{j,\bullet} = (N_{j,0}, \dots, N_{j,D-1})$ , with  $N_{j,d} = \det((\nabla_{\xi} \mathbf{X})(d | \vec{e}^j))$ ,  $d = 0, \dots, D-1$ , defines a vector field on  $\mathbb{R}^D$  with the corresponding  $(D-1)$ -form:

$$w_j = N_{j,0} (dx^1 \wedge dx^2 \wedge \cdots \wedge dx^{D-1}) + \cdots + (-1)^{D-1} N_{j,D-1} (dx^0 \wedge dx^1 \wedge \cdots \wedge dx^{D-2})$$

Since the rows of  $N$  are divergence free, the exterior derivative of  $w_j$  is

$$dw_j = \text{div}(N_{j,\bullet}) (dx^0 \wedge dx^1 \wedge \cdots \wedge dx^{D-1}) = 0$$

Now, we assume that the faces  $A_{\pm}^d$  and  $A_{EB}$  are or can be represented as a star-shaped with respect to zero, where:

**DEFINITION 5.1.** *An open set  $A \subset \mathbb{R}^D$  is called star-shaped with respect to 0, if for any  $x \in A$  the line segment from 0 to  $x$  is contained in  $A$ .*

Therefore, according to the following theorem:

**THEOREM 5.1 (Poincare Lemma).** *Let  $A \subset \mathbb{R}^D$  be a star-shaped with respect to 0. If  $w$  is a closed form on  $A$  ( $dw = 0$ ) then  $w$  is exact that is,  $w = d\eta$ , for some  $\eta$ ;*

there exist a  $(D - 2)$ -form,  $\eta_j$ , such as

$$w_j = d\eta_j$$

Example: In 2D the matrix  $N$  is given by

$$N = \begin{pmatrix} \frac{\partial X_1}{\partial \xi_1} & -\frac{\partial X_1}{\partial \xi_0} \\ -\frac{\partial X_0}{\partial \xi_1} & \frac{\partial X_0}{\partial \xi_0} \end{pmatrix}$$

Each row of  $N$  defines a vector field. The first row, for instance, is equal to

$$N_{0,\bullet} = \left( \frac{\partial X_1}{\partial \xi_1}, -\frac{\partial X_1}{\partial \xi_0} \right)$$

The corresponding 1-form is

$$w_0 = \frac{\partial X_1}{\partial \xi_1} d\xi_1 + \frac{\partial X_1}{\partial \xi_0} d\xi_0,$$

and

$$dw_0 = \text{div}(N_{0,\bullet}) (dx^0 \wedge dx^1) = \left( \frac{\partial^2 X_1}{\partial \xi_0 \partial \xi_1} - \frac{\partial^2 X_1}{\partial \xi_1 \partial \xi_0} \right) (dx^0 \wedge dx^1) = 0,$$

assuming  $X_1$  is, at least,  $C^2$ . Thus, according to theorem 5.1, there exist a 0-form, i.e., a smooth function,  $\eta_0$ , such as

$$\frac{\partial X_1}{\partial \xi_1} d\xi_1 + \frac{\partial X_1}{\partial \xi_0} d\xi_0 = w_0 = d\eta_0 = \frac{\partial \eta_0}{\partial \xi_0} d\xi_0 + \frac{\partial \eta_0}{\partial \xi_1} d\xi_1$$

For this particular example we clearly see that  $\eta_0 = X_1$ .

The form  $\eta$  is not unique. In this work we follow the formulas given in [1], where each entry,  $N_{j d}$ , of  $N$  can be written as:

$$N_{j d} = \sum_{\substack{s=0, \dots, D-1 \\ s \neq d}} \frac{\partial N_{j d}^s}{\partial \xi_s},$$

with

$$N_{j d}^s = \frac{1}{D-1} \det[(\nabla_\xi \mathbf{X})(\mathbf{X} | j)(s | \vec{e}^d)] \quad (5.14)$$

If we define  $\hat{N}_{j d} = (N_{j d}^0, N_{j d}^1, \dots, N_{j d}^{d-1}, N_{j d}^{d+1}, \dots, N_{j d}^{D-1})$  then, we can write

$$\int_{A_\pm^d} N_{j d} dA_\xi = \int_{A_\pm^d} \nabla \cdot \hat{N}_{j d} dA_\xi = \sum_{\substack{s=0 \\ s \neq d}}^{D-1} \sum_{\hat{\pm}=+,-} \hat{\pm} \int_{(A_\pm^d)_{\hat{\pm}}^s} N_{j d}^s dE_\xi + \int_{(A_\pm^d)_{EB}} \hat{N}_{j d} \cdot \hat{n} dE_\xi$$

where the last equality is a consequence of the divergence theorem,  $(A_\pm^d)_{\hat{\pm}}^s$  is the edge of the face  $A_\pm^d$  in the  $s$  direction, and  $(A_\pm^d)_{EB}$  is the intersection of the domain  $\Omega$  with  $A_\pm^d$ .

On the other hand, if  $B_\pm^d$  denotes the face-complement of  $A_\pm^d$  over the rectangular control volume  $\Upsilon_i$ , by using the fact that the rows of  $N$  are divergence free and after applying the divergence theorem, we have that:

$$0 = \int_{\Upsilon_i - V_i} \nabla_\xi \cdot (N_{j, \bullet}) d\xi = \sum_{d=0}^{D-1} \sum_{\pm=+,-} \pm \int_{B_\pm^d} N_{j d} dA_\xi + \int_{A_{EB}} (N \hat{n})_j dA_\xi$$

Thus,

$$\int_{A_{EB}} (N \hat{n})_j dA_\xi = - \sum_{d=0}^{D-1} \sum_{\pm=+,-} \pm \int_{B_\pm^d} N_{j d} dA_\xi = - \sum_{d=0}^{D-1} \sum_{\pm=+,-} \pm \int_{B_\pm^d} \nabla \cdot \hat{N}_{j d} dA_\xi$$

$$\begin{aligned} \int_{A_{EB}} (N \hat{n})_j dA_\xi = & \\ & - \sum_{d=0}^{D-1} \sum_{\pm=+,-} \pm \left[ \sum_{\substack{s=0 \\ s \neq d}}^{D-1} \sum_{\hat{\pm}=+,-} \hat{\pm} \int_{(B_\pm^d)_{\hat{\pm}}^s} N_{j d}^s dE_\xi + \int_{(A_\pm^d)_{EB}} \hat{N}_{j d} \cdot \hat{n} dE_\xi \right] \end{aligned}$$

where  $(B_{\pm}^d)_{\pm}^s$  is the edge of the face  $B_{\pm}^d$  in the  $s$  direction.

The different integrals over  $(A_{\pm}^d)_{\pm}^s$ ,  $(B_{\pm}^d)_{\pm}^s$ , and  $(A_{\pm}^d)_{EB}$  are calculated using quadratures, with the convention that the same quadrature rule is used wherever the integrals appear.

We finish this section showing an algorithm for computing  $N_{j^s_d}$  when  $D = 3$ , suitable for coding purposes, namely

$$N_{j^s_d} = \frac{(-1)^{j+d}}{2} \left[ (-1)^k X_n \frac{\partial X_m}{\partial \xi_l} + (-1)^{k+1} X_m \frac{\partial X_n}{\partial \xi_l} \right], \quad (5.15)$$

where  $k = 0$  if  $l < s$  or  $k = 1$  otherwise,  $m = \min(d_1, d_2)$ ,  $n = \max(d_1, d_2)$ ,  $l \neq s, d$ , and  $j \neq d_1, d_2$ .

## 6. Mapped grid Embedded Boundary Method.

The resulting formula for calculating the divergence-average over the control volume  $V_i$  for the Mapped Embedded Boundary case, is given by:

$$\int_{V_i} \nabla_{\xi} \cdot (N^T \mathbf{F}) d\xi = \quad (6.1)$$

$$\sum_{d=0}^{D-1} \sum_{\pm=+,-} \pm \left[ \int_{A_{\pm}^d} \sum_{1 \leq |p| \leq P} \frac{1}{p!} (\xi - \xi_{\pm}^d)^p \sum_{\substack{j=0, \dots, D-1 \\ 0 \leq |q| \leq |p|-1}} K_q \nabla^{p-q, q} (\mathbf{F}_j, N_{d^j}^T) (\xi_{\pm}^d) dA_{\xi} \right] \quad (6.1.a)$$

$$+ \sum_{j=0}^{D-1} \mathbf{F}_j(\xi_{\pm}^d) \left[ \sum_{\substack{s=0 \\ s \neq d}}^{D-1} \sum_{\pm=+,-} \hat{\pm} \int_{(A_{\pm}^d)_{\pm}^s} N_{j^s_d} dE_{\xi} + \int_{(A_{\pm}^d)_{EB}} \hat{N}_{j^s_d} \cdot \hat{n} dE_{\xi} \right] \quad (6.1.b)$$

$$+ \sum_{s=0}^{D-1} \int_{A_{EB}^s} \left[ \sum_{1 \leq |p| \leq P} \frac{1}{p!} (\xi - \xi_{EB})^p \sum_{\substack{j=0, \dots, D-1 \\ 0 \leq |q| \leq |p|-1}} K_q \nabla^{p-q, q} (\mathbf{F}_j, N_{s^j}^T) (\xi_{EB}) \right] \hat{n}_s dA_{\xi} \quad (6.1.c)$$

$$- \sum_{j=0}^{D-1} \left[ \mathbf{F}_j(\xi_{EB}) \sum_{d=0}^{D-1} \sum_{\pm=+,-} \pm \left[ \sum_{\substack{s=0 \\ s \neq d}}^{D-1} \sum_{\pm=+,-} \hat{\pm} \int_{(B_{\pm}^d)_{\pm}^s} N_{j^s_d} dE_{\xi} + \int_{(A_{\pm}^d)_{EB}} \hat{N}_{j^s_d} \cdot \hat{n} dE_{\xi} \right] \right] \quad (6.1.d)$$

$$+ O(h^{P+D})$$

where  $\hat{N}_{j^s_d} = (N_{j^0_d}^0, N_{j^1_d}^1, \dots, N_{j^{d-1}_d}^{d-1}, N_{j^{d+1}_d}^{d+1}, \dots, N_{j^{D-1}_d}^{D-1})$  and  $N_{j^s_d}$  are given by equations (5.14) or (5.15) if  $D = 3$ .

## 7. Particular cases obtained from equation (6.1).

As shown in this section, from expression (6.1) we can also obtain formulas for the particular cases Cartesian EB and Mapped FV.

### 7.1. Cartesian grid Embedded Boundary Method.

The analysis presented in previous pages also holds for the Cartesian EB case, which, after all, it's a mapped EB problem with the mapping being the identity operator.

By using formula (6.1) with  $N$  equal the identity matrix, we get the following high-order, conservative, freestream preserving scheme:

$$\int_{V_i} \nabla_{\xi} \cdot F dx = \tag{7.1}$$

$$\sum_{d=0}^{D-1} \sum_{\pm=+,-} \pm \left[ \sum_{1 \leq |p| \leq P} \frac{1}{p!} \nabla^p F_d(x_{\pm}^d) \int_{A_{\pm}^d} (x - x_{\pm}^d)^p dA_x \right. \tag{7.1.a}$$

$$\left. + \sum_{j=0}^{D-1} F_j(x_{\pm}^d) \left[ \sum_{\substack{s=0 \\ s \neq d}}^{D-1} \sum_{\hat{\pm}=+,-} \hat{\pm} \int_{(A_{\pm}^d)_{\hat{\pm}}} N_{j,d}^s dE_x + \int_{(A_{\pm}^d)_{EB}} \hat{N}_{j,d} \cdot \hat{n} dE_x \right] \right] \tag{7.1.b}$$

$$+ \sum_{s=0}^{D-1} \int_{A_{EB}} \left[ \sum_{1 \leq |p| \leq P} \frac{1}{p!} (x - x_{EB})^p \nabla^p F_s(x_{EB}) \right] \hat{n}_s dA_x \tag{7.1.c}$$

$$- \sum_{j=0}^{D-1} \left[ F_j(x_{EB}) \sum_{d=0}^{D-1} \sum_{\pm=+,-} \pm \left[ \sum_{\substack{s=0 \\ s \neq d}}^{D-1} \sum_{\hat{\pm}=+,-} \hat{\pm} \int_{(B_{\pm}^d)_{\hat{\pm}}} N_{j,d}^s dE_x + \int_{(A_{\pm}^d)_{EB}} \hat{N}_{j,d} \cdot \hat{n} dE_x \right] \right] \tag{7.1.d}$$

$$+ O(h^{P+D})$$

### 7.2. Mapped Finite Volume Method.

When we have a boundary conforming, curvilinear mesh, formula (6.1) produces the high-order, conservative, freestream preserving Finite Volume method:

$$\int_{V_i} \nabla_{\xi} \cdot (N^T \mathbf{F}) d\xi = \quad (7.2)$$

$$\sum_{d=0}^{D-1} \sum_{\pm=+,-} \pm \left[ \int_{A_{\pm}^d} \sum_{1 \leq |p| \leq P} \frac{1}{p!} (\xi - \xi_{\pm}^d)^p \sum_{\substack{j=0, \dots, D-1 \\ 0 \leq |q| \leq |p|-1}} K_q \nabla^{p-q, q} (\mathbf{F}_j, N_{dj}^T)(\xi_{\pm}^d) dA_{\xi} \right] \quad (7.2.a)$$

$$+ \sum_{j=0}^{D-1} \mathbf{F}_j(\xi_{\pm}^d) \left[ \sum_{\substack{s=0 \\ s \neq d}}^{D-1} \sum_{\hat{\pm}=+,-} \hat{\pm} \int_{(A_{\pm}^d)_{\hat{\pm}}^s} N_{jd}^s dE_{\xi} \right] \quad (7.2.b)$$

$$+ O(h^{P+D}),$$

## 8. Numerical Results.

### Mapped EB

In this example we have implemented a fourth order, mapped embedded boundary scheme (formula (6.1)). That is,  $P$  is equal to 2 in (6.1), the normal vector has been Taylor-expanded with a second order polynomial, and the moments are computed with fourth order accuracy.

We consider the flux:

$$\mathbf{F}(\xi) = (2\pi \cos(2\pi \xi_0) \sin(2\pi \xi_1), 2\pi \sin(2\pi \xi_0) \cos(2\pi \xi_1))^T,$$

and a curvilinear grid given by the map:

$$X(\xi) = (\xi_0, \xi_1 + 2\xi_1^2(1 - \xi_1)^2 \sin(2\pi \xi_0))^T$$

The domain (blue region) and an example of the mesh are shown in figure 8.1.

Errors, computed in three different norms, are shown in figure 8.2. We see we get fourth order accuracy in  $L_2$ -norm and third in Max-norm. Thus, at cut cells we lose one order of accuracy.

We also checked for freestream preservation by considering the same topology but, taking the flux to be constant. Results are shown in table 8.1. We see exact zero, up to machine precision, is obtained.

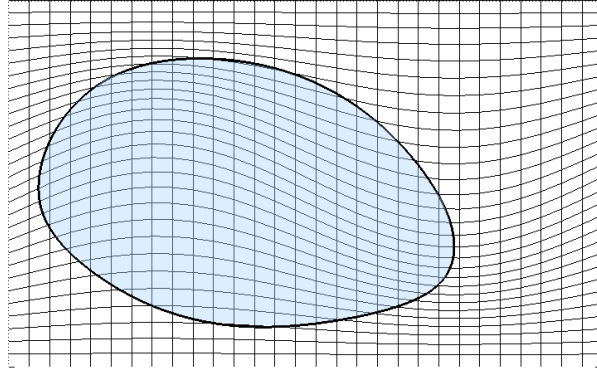


FIG. 8.1. *Non-symmetric domain and an example of the curvilinear grid with  $30 \times 30$  nodes. The grid inside the domain is also non-symmetric with respect to the domain.*

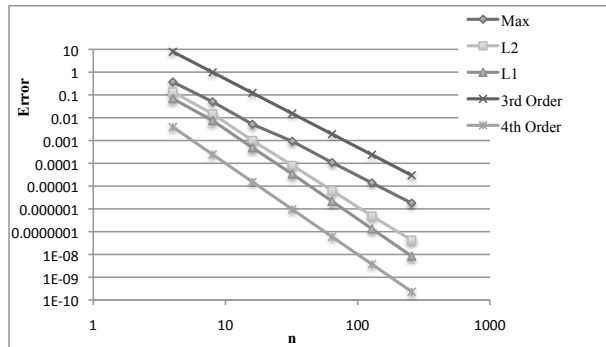


FIG. 8.2. *Error. We have drawn third and fourth order lines for reference*

TABLE 8.1  
*Freestream preservation*

$N_{points}$	$\  \cdot \ _1$
4	$8.88 \times 10^{-16}$
8	$4.44 \times 10^{-16}$
16	$2.77 \times 10^{-16}$
32	$1.31 \times 10^{-16}$
64	$8.33 \times 10^{-17}$
128	$5.55 \times 10^{-17}$
256	$2.78 \times 10^{-17}$
512	$2.008 \times 10^{-17}$

Cartesian EB

In this example we have implemented a fourth order, Cartesian embedded boundary method.

We consider the flux:

$$F(\xi) = (2\pi \cos(2\pi \xi_0) \sin(2\pi \xi_1), 2\pi \sin(2\pi \xi_0) \cos(2\pi \xi_1))^T,$$

and the map to be the identity operator,  $X(\xi) = \xi$ .

The domain (blue region) and an example of the mesh are shown in figure (8.3).

Errors, computed in three different norms, are shown in figure (8.4). We get fourth order accuracy in  $L_2$ -norm and third in Max-norm. As before, we lose one order of accuracy at cut cells.

We checked for freestream preservation by considering a constant flux under the same topology. Results are shown in table (8.2), where we see exact zero, up to machine precision.

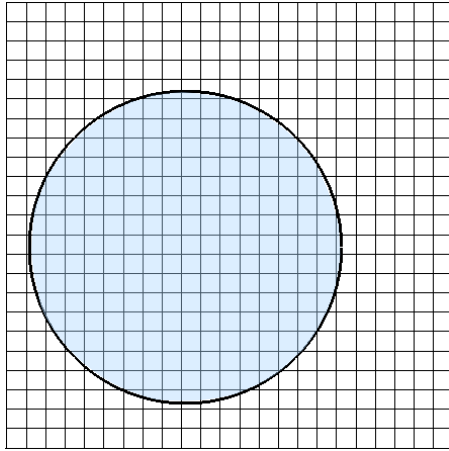


FIG. 8.3. Domain (blue region) and a Cartesian cut cell grid.

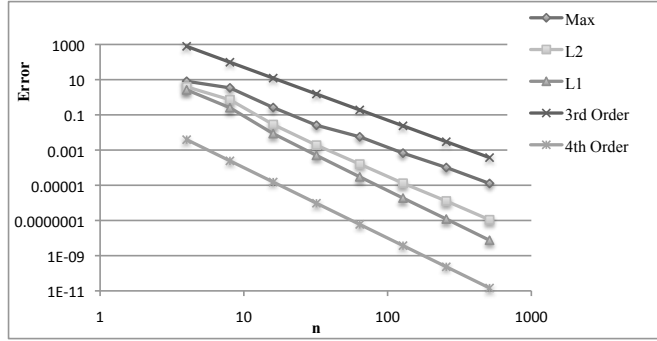


FIG. 8.4. Error. We have drawn third and fourth order lines for reference

TABLE 8.2  
Freestream preservation

$N_{points}$	$\  \cdot \ _1$
4	$4.44 \times 10^{-16}$
8	$4.44 \times 10^{-16}$
16	$2.22 \times 10^{-16}$
32	$1.11 \times 10^{-16}$
64	$6.26 \times 10^{-17}$
128	$3.12 \times 10^{-17}$
256	$1.73 \times 10^{-17}$
512	$1.04 \times 10^{-17}$

### Mapped FV

In this example we have implemented a second order, mapped finite volume method.

We consider the flux:

$$F(\xi) = (2\pi \cos(2\pi \xi_0) \sin(2\pi \xi_1), 2\pi \sin(2\pi \xi_0) \cos(2\pi \xi_1))^T,$$

and a curvilinear grid given by the map:

$$X(\xi) = (1.7 + (0.148 \xi_0 + 0.462) \cos(2\pi \xi_1) + 0.429 \sin(2\pi \xi_1), \\ 1.66(0.148 \xi_0 + 0.462) \sin(2\pi \xi_1))^T$$

The domain (blue region) and an example of the mesh are shown in figure (8.5).

Errors, computed in three different norms, are shown in figure (8.6). We see we get second order accuracy in all norms:  $L_1$ ,  $L_2$ , and Max norm.

For this particular example we can easily checked for conservation since the flux is equal to zero at the boundary of the domain. As shown in table (8.3), we observe

exact conservation, up to machine precision.

Finally, we also checked for freestream preservation by considering the same topology but, taking the flux to be constant. Results are shown in table (8.4), where we see exact zero, up to machine precision.

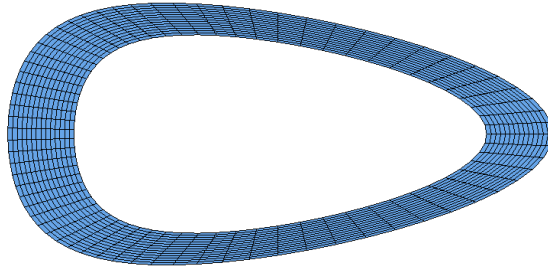


FIG. 8.5. Domain (blue region) and a boundary conforming curvilinear grid.

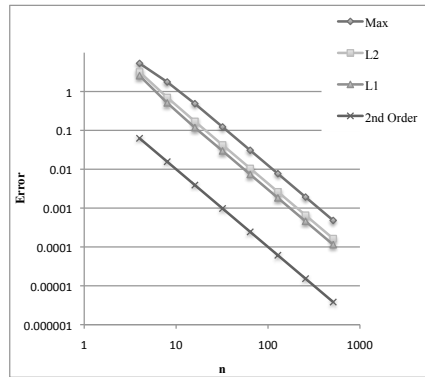


FIG. 8.6. Error. We have drawn a second order line for reference

TABLE 8.3  
Conservation

$N_{points}$	Sum of $\langle \nabla_x \cdot F \rangle$
4	$1.78 \times 10^{-15}$
8	$-3.33 \times 10^{-15}$
16	$-2.83 \times 10^{-15}$
32	$7.91 \times 10^{-16}$
64	$-5.03 \times 10^{-17}$
128	$2.75 \times 10^{-16}$
256	$1.05 \times 10^{-15}$
512	$1.86 \times 10^{-15}$

TABLE 8.4  
*Freestream preservation*

$N_{points}$	$\  \cdot \ _1$
4	$2.88 \times 10^{-15}$
8	$2.10 \times 10^{-15}$
16	$1.16 \times 10^{-15}$
32	$8.12 \times 10^{-16}$
64	$4.44 \times 10^{-16}$
128	$2.64 \times 10^{-16}$
256	0
512	$1.43 \times 10^{-16}$

### Mapped FV - 3D

In our last example we have implemented a second order, mapped finite volume scheme in 3D.

We consider the flux:

$$F(\xi) = \begin{pmatrix} 2\pi \cos(2\pi \xi_0) \sin(2\pi \xi_1) \sin(2\pi \xi_2), \\ 2\pi \sin(2\pi \xi_0) \cos(2\pi \xi_1) \cos(2\pi \xi_2), \\ \xi_2 \end{pmatrix}^T$$

and a curvilinear grid given by the map:

$$X(\xi) = \left( 5\xi_0, \frac{\xi_1}{2}, \frac{\xi_2}{4} \right)^T$$

The domain (blue region) and an example of the mesh are shown in figure (8.7).

Errors, computed in three different norms, are shown in figure (8.8). We get third order accuracy in all norms:  $L_1$ ,  $L_2$ , and Max norm, even though we have implemented a second order scheme. Since the mesh is orthogonal, we think we are getting some extra cancellations in the error term.

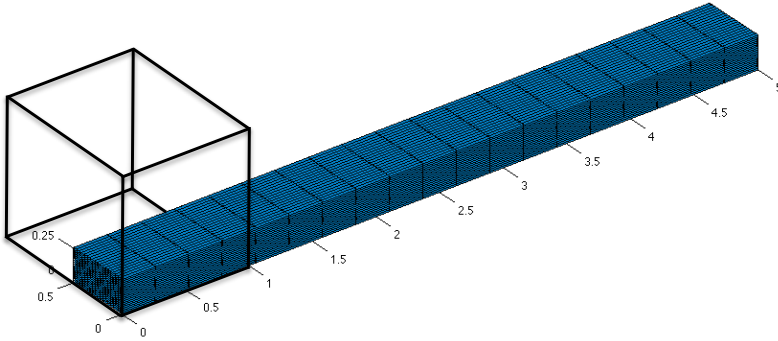


FIG. 8.7. Domain (blue region) and a boundary conforming grid in 3D.

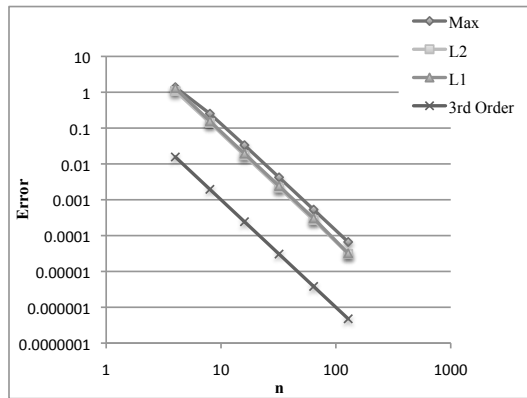


FIG. 8.8. Error. We have drawn a third order line for reference

## 9. Summary.

- We have presented an Embedded Boundary Scheme in Mapped Coordinates that is high-order, multi-dimensional, conservative, and freestream preserving.
- This formulation reduces to the scheme presented in [1] when a boundary conforming mesh is used.
- We show why by just taking Taylor expansions we fail to obtain freestream preservation and how to fix this, a theoretical result which is one of the main contribution of this report.
- The second main contribution has been the construction of an exact formula for calculating multi-dimension derivatives of product of functions.
- The analysis presented here is quite general, covering the cases Finite Volume, Cartesian grid Embedded Boundary, and Mapped grid Embedded Boundary as well.

- By taking  $X$  equals the identity map, we get a Cartesian grid EB method that is freestream preserving.
- A key factor for having a conservative scheme was to take Taylor expansions at faces centroids.
- Key factors for having freestream preservation were the use of the new formula for multi-dimension derivatives (5.13) and the use of (Poincaré) lemma 5.1.

**Acknowledgments.** P. Colella, T. Ligocki, and P. Schwartz. Thanks to the Advanced Numerical Algorithms Group, for all the enlightening discussions we had. This project was entirely founded by the US Department of Energy.

#### REFERENCES

- [1] P. COLELLA, M. R. DORR, J. A. F. HITTINGER, AND D. F. MARTIN, *High-order, finite-volume methods in mapped coordinates*, J. Comput. Phys., 230 (2011), pp. 2952–2976.
- [2] J. LOUGHRY, J. I. VAN HEMERT, AND L. SCHOofs, *Efficiently enumerating the subsets of a set*, (2000), pp. 1–10.
- [3] P. COLELLA, D. GRAVES, T. LIGOCKI, D. TREBOTICH, AND B. VAN STRAALEN, *Embedded boundary algorithms and software for partial differential equations*, J. of Phys.: Conference series, 125 (2008), doi:10.1088/1742-6596/125/1/012084.
- [4] T. J. LIGOCKI, P. O SCHWARTZ, J. PERCELAY, AND P. COLELLA, *Embedded boundary grid generation using the divergence theorem, implicit functions, and constructive solid geometry*, J. Comput. Phys.: Conference series, 125 (2008), doi:10.1088/1742-6596/125/1/012080.
- [5] D. TREBOTICH, B. VAN STRAALEN, D. GRAVES, AND P. COLELLA, *Performance of embedded boundary methods for CFD with complex geometry*, J. of Phys.: Conference series, 125 (2008), doi:10.1088/1742-6596/125/1/012083.
- [6] P. COLELLA, D. GRAVES, B. J. KEEN, D. MODIANO, *A Cartesian grid embedded boundary method for hyperbolic conservation laws*, J. Comput. Phys., 211 (2006), pp. 347–366.
- [7] P. SCHWARTZ, M. BARAD, P. COLELLA, AND T. LIGOCKI, *A Cartesian grid embedded boundary method for the heat equation and Poisson's equation in three dimensions*, J. Comput. Phys., 211 (2006), pp. 531–550.
- [8] M. BARAD AND P. COLELLA, *A fourth-order accurate local refinement method for Poisson's equation*, J. Comput. Phys., 209 (2005), pp. 1–18.
- [9] P. MCCORQUODALE, P. COLELLA, AND H. JOHANSEN, *A Cartesian grid embedded boundary method for the heat equation on irregular domains*, J. Comput. Phys., 173 (2001), pp. 620–635.
- [10] H. JOHANSEN AND P. COLELLA, *A Cartesian grid embedded boundary method for Poisson's equation on irregular domains*, J. Comput. Phys., 147 (1998), pp. 60–85.